LOADING AND CURLING STRESS MODELS FOR CONCRETE PAVEMENT DESIGN

By Ying-Haur Lee[1] and Michael I. Darter[2]

ABSTRACT

The determination of the edge loading tensile bending stress in a concrete slab due to individual and combination effects of wheel loading and thermal curling is important to a mechanistic based design procedure. This paper first presents the recent discovery of two additional dimensionless mechanistic variables such that the problems encountered in previous investigations using dimensional analysis for thermal-related curling problems are resolved. A new regression technique (projection pursuit regression) together with traditional linear and nonlinear regressions are utilized to develop prediction models. These prediction models provide an accurate representation of the finite element model. They are simple, easy to comprehend, dimensionally correct, may be extrapolated to wider ranges of other input parameters and are ready for implementation in a spreadsheet or computer program. Practical application examples showing the use of the new models are also provided.

KEY WORDS

concrete pavement, stress analysis, wheel loading, thermal curling, dimensional analysis, predictive modeling, projection pursuit regression (PPR), mechanistic design models.

---

[1] Associate Professor, Department of Civil Engineering, Tamkang University; E725, #151, Ying-Chuan Rd., Tamsui, Taipei, Taiwan 25137, R.O.C.; TEL: (886-2) 623-4380; FAX: (886-2) 620-2193.

[2] Professor of Civil Engineering, University of Illinois; NCEL #1212, 205 N. Mathews Ave., Urbana, IL 61801, U.S.A.; TEL: (217) 333-6253; FAX: (217) 333-9464

INTRODUCTION

Cracking of slabs can be caused by three different repeated loading positions: transverse joint, longitudinal joint midway between transverse joints and at the corner. Given certain design, construction and loading conditions, any of these load positions could lead to fatigue cracking over time. This paper focuses on the longitudinal joint edge location which could lead to transverse cracking. The determination of the maximum bending stress at the edge is important to a mechanistic based design procedure (the other positions are also very important and should be evaluated). The analysis of longitudinal edge stress due to the individual and combination effects of wheel loading and thermal curling is presented in this paper. Critical stresses from the corner loading is being pursued as part of continuing research at the University of Illinois.

Finite element models have been successfully utilized to account for the effects of a finite slab size as well as possible loss of support due to a linear temperature differential more realistically than theoretical solutions based on infinite slab and full contact assumptions. However, due to the required run time and complexity of the finite element model, finite element analysis can not be easily implemented as a part of a design procedure. Therefore, a series of finite element runs were performed over a wide range of pavement designs. The resulting edge stresses were compared to theoretical Westergaard solutions and adjustment factors were introduced to account for this discrepancy. Statistical regression techniques were utilized to develop predictive models for each adjustment factor. These predictive models were then used as an alternative to finite element analysis to estimate stresses for pavement design with sufficient accuracy.

Previous predictive models (*1, 2*) were based on a series of input parameters using multiple regression and/or stepwise regression techniques. Thus, the resulting models contain only arbitrary linear combinations of variables with very few insights in describing their actual physical relationships. The results of the prediction are also limited to the ranges of the cases analyzed.

This paper presents a more mechanistic-based approach in developing such predictive models. Through the use of the principles of dimensional analysis, the dominating mechanistic variables were first identified based on previous research. In addition, two newly discovered additional dimensionless mechanistic variables were necessary such that the problems encountered in previous investigations using dimensional analysis for thermal-related curling problems are resolved. A new regression technique (projection pursuit regression) together with traditional linear and nonlinear regressions were utilized to develop prediction models.

Consequently, three closed-form mechanistic design models which have been carefully validated and ready for implementation in a spreadsheet or computer program are presented as a result of this study. In contrast to those earlier predictive models, the new models not only used only the dominating mechanistic variables identified herein, but they were also properly formulated to satisfy applicable engineering boundary conditions. These stress models turned out to be very accurate representations of the finite element model. They are simple, easy to comprehend, dimensionally correct, and may be extrapolated to wider ranges of other input parameters. The parameter estimates of each model have their own physical meanings as well. Practical application examples showing the use of the new models are also provided.

This paper not only provides more complete coverage of the solutions to the cases analyzed, but it also demonstrates the advantages of incorporating subject-related engineering knowledge and selecting proper functional forms for the predictive models. This paper will be of interest to those working on mechanistic pavement design and pavement prediction modeling.

IDENTIFICATION OF IMPORTANT MECHANISTIC VARIABLES

Primary Structural Responses Due to Loading

In the analysis of a slab-on-grade pavement system, Westergaard (*3, 4, 5*) has presented closed-form solutions for three primary structural response variables, i.e., slab bending stress, slab deflection, and subgrade stress, due to a single wheel load. Based on the assumptions of an infinite or semi-infinite slab over a dense liquid foundation (Winkler foundation), three different loading conditions (interior, edge, and corner) were analyzed. The Westergaard solutions for a circular edge loading based on medium-thick plate theory are given as follows:

$$\sigma_w = \frac{3(1+\mu)P}{\pi(3+\mu)h^2}\left[\log_e \frac{Eh^3}{100ka^4} + 1.84 - \frac{4\mu}{3} + \frac{1-\mu}{2} + 1.18(1+2\mu)\frac{a}{l}\right] \quad \textbf{(1)}$$

$$\delta_w = \frac{\sqrt{2+1.2\mu}\,P}{\sqrt{Eh^3k}}\left[1 - (0.76+0.4\mu)\frac{a}{l}\right] \quad \textbf{(2)}$$

$$l = \sqrt[4]{\frac{Eh^3}{12(1-\mu^2)k}} \quad \textbf{(3)}$$

Where:

σ_w = Westergaard's edge stress, [FL^{-2}];

δ_w = Westergaard's edge deflection, [L];

P = total applied wheel load [F];

a = radius of the applied circular load [L];

E = modulus of elasticity of the concrete slab [FL^{-2}];

h = thickness of the slab [L];

μ = Poisson's ratio of the concrete;

k = modulus of subgrade reaction [FL^{-3}]; and

l = radius of relative stiffness of the slab subgrade system [L].

(Note: Primary dimensions are represented by [F] for force and [L] for length.)

The subgrade stress was not explicitly specified, however, it can be easily determined by multiplying the slab deflection by the modulus of subgrade reaction.

Through the use of the principles of dimensional analysis, earlier investigators (*6*) have demonstrated that theoretical Westergaard solutions for these three primary structural responses can be reduced to three dimensionless terms shown as follows, which all depend on the normalized load radius alone for a constant Poisson's ratio (usually $\mu \approx 0.15$).

$$\frac{\sigma h^2}{P}, \frac{\delta k l^2}{P}, \frac{q l^2}{P} = f\left(\frac{a}{l}\right) \quad \textbf{(4)}$$

Where:

σ, q = slab bending stress and subgrade vertical stress, respectively, [FL^{-2}]; and

δ = slab deflection, [L].

By doing so, the relationships between the primary structural responses and the external wheel loading are concisely defined. The dependent variables are $\sigma h^2/P$, $\delta k l^2/P$, and $q l^2/P$, whereas independent variable is the dominating factor a/l, rather than the other input parameters (E, h, μ, k, and a). These relationships are not only simple to understand, but they also provide a dimensionally correct form for further analysis on a more complicated problem.

The analysis of finite slab length and width effect due to an external wheel load is not possible until the introduction of finite element models. According to previous research (*6, 7*), the normalized slab length and width (L/l and W/l) are the dominating mechanistic variables for the finite extent of slab condition, where L and W are the finite slab length and width, respectively. In fact, theoretical treatments on the effect of thermal curling (rather than wheel loading), which can be traced back as early as Westergaard (*8*) and Bradbury (*9*), have already shown that the finite extent of slab condition is simply a function of these two dimensionless terms. Thus, the following expression can concisely describe the above relationships:

$$\frac{\sigma h^2}{P}, \frac{\delta k l^2}{P}, \frac{q l^2}{P} = f\left(\frac{a}{l}, \frac{L}{l}, \frac{W}{l}\right) \quad \textbf{(5)}$$

Primary Structural Responses Due to Thermal Curling

Considering curling stresses caused by a linear temperature differential on a concrete slab over a dense liquid foundation, Westergaard (*8*) developed equations for three slab conditions (i.e., infinite, semi-infinite, and an infinite long strip). For the case of an infinitely long strip which had a finite width W and an infinite length along x axis. The deflection and bending stress solutions along the y axis are given as follows:

$$\sigma_y = \sigma_0 \{1 - \frac{2\cos\lambda\cosh\lambda}{\sin 2\lambda + \sinh 2\lambda} [(\tan\lambda + \tanh\lambda) \cos\frac{y}{l\sqrt{2}} \cosh\frac{y}{l\sqrt{2}} + (\tan\lambda - \tanh\lambda) \sin\frac{y}{l\sqrt{2}} \sinh\frac{y}{l\sqrt{2}}] \} \tag{6}$$

$$\delta_y = -\delta_0 \frac{2\cos\lambda\cosh\lambda}{\sin 2\lambda + \sinh 2\lambda} [(-\tan\lambda + \tanh\lambda) \cos\frac{y}{l\sqrt{2}} \cosh\frac{y}{l\sqrt{2}} + (\tan\lambda + \tanh\lambda) \sin\frac{y}{l\sqrt{2}} \sinh\frac{y}{l\sqrt{2}}] \tag{7}$$

$$\sigma_0 = \frac{E\alpha\Delta T}{2(1-\mu)} \quad , \quad \delta_0 = \frac{(1+\mu)\,\alpha\,\Delta T\, l^2}{h} \quad , \quad \lambda = \frac{W}{l\sqrt{8}} \tag{8}$$

Where:

σ_y = bending stress along the y axis, (y is equal to ± W/2 at the slab edges) [FL^{-2}];

δ_y = deflection along the y axis, [L];

α = thermal expansion coefficient of the concrete slab, [T^{-1}]; and

ΔT = linear temperature differential through the thickness of the slab, [T].

Bradbury (*9*) later expanded the Westergaard's bending stress solutions for a slab with finite dimensions in both x and y directions. Thus, considering a very narrow and long strip of slab, the curling stress along the very edge of the slab could be determined by the following equation:

$$\sigma_c = \frac{CE\alpha\Delta T}{2} = \frac{E\alpha\Delta T}{2}\left[1 - \frac{2\cos\lambda\cosh\lambda}{\sin 2\lambda + \sinh 2\lambda}\left(\tan\lambda + \tanh\lambda\right)\right] \tag{9}$$

Where: σ_c = bending stress at the edge of the slab due to thermal curling, [FL^{-2}].

Similarly, the closed-form solutions derived for slab bending stress, slab deflection, and subgrade stress due to a linear temperature differential can be summarized in the following expression using dimensional analysis for a constant Poisson's ratio:

$$\frac{\sigma}{E} , \frac{\delta h}{l^2} , \frac{qh}{kl^2} = f\left(\alpha\Delta T , \frac{L}{l} , \frac{W}{l}\right) \tag{10}$$

Two Additional Dimensionless Parameters Identified

For thermal-related curling problems, Westergaard/Bradbury's analytical solutions are based on a full contact assumption between the pavement slab and the subgrade. However, experimental data by Teller and Sutherland (*10*) have clearly shown that parts of the pavement slab were found without subgrade support when a temperature or moisture differential existed through the slab thickness. Thus, the effect of the loss of subgrade support due to a temperature differential has to be considered in order to more realistically account for the actual pavement condition. The ILLI-SLAB finite element model (*11, 12, 13*), which has implemented this effect through an iterative procedure and has been developed over the years at the University of Illinois, was selected for this study.

Because of the above theoretical difference, attempts by earlier investigators (*1*) to relate the actual structural response due to the combination effect of a single wheel load and a temperature influence using only the aforementioned dimensionless parameters were not very successful. Thus, it was necessary to search for other possible mechanistic variables to adequately describe this difference. Particular attention was focused on the effect of the self-weight of the concrete slab on the thermal-induced curling stress. Westergaard (*8*) did not explicitly consider the self-weight effect in his deflection equation, since the center of the slab was assumed to be flat and the deflection was zero. On the other hand, the effect of self-weight is included in the ILLI-SLAB model. The deflection at the center is determined by:

$$\delta_{\gamma} = \frac{\gamma h}{k} \tag{11}$$

Where: γ = unit weight of the concrete slab, [FL^{-3}].

Considering Westergaard's analytical solution for deflection as shown in equation (7), the deflection due to thermal curling alone may be described by normalized slab length and width (L/l and W/l), the dimensionless product of $\alpha\Delta T$, and the deflection factor (l^2/h). All these parameters are dimensionless except the last one, l^2/h, which has the same dimension as length and can be used as an indicator for the extent of loss of subgrade support. By taking the ratio of self-weight deflection versus l^2/h, the following dimensionless parameter, D_γ, was defined to represent the relative deflection stiffness due to the self-weight of the concrete slab and the possible loss of subgrade support:

$$D_\gamma = \frac{\gamma h^2}{k l^2} \tag{12}$$

It was hypothesized that the resulting ILLI-SLAB edge strain due to curling alone may be well characterized by L/l, W/l, $\alpha\Delta T$, as well as this additional parameter (D_γ). To validate this hypothesis, 16 ILLI-SLAB runs were performed by keeping the above four parameters constant while changing any individual input variables. The resulting edge stress was numerically confirmed to be proportional to the elastic modulus of the concrete slab as summarized in Table 1. In other words, the resulting edge strains are equal to each other.

By the same token, this "deflection-ratio" concept was applied again in searching for another dimensionless parameter for the effect of an applied wheel loading on a curled slab due to a linear temperature differential. Based on the Westergaard's analytical solution for deflection as shown in equation (2), the edge deflection can be represented by two parameters, a/l and $P/(Eh^3k)^{1/2}$. The second one is a deflection factor which is analogous to P/kl^2 and has the same dimension as length. By taking the ratio of this deflection factor versus l^2/h, the following dimensionless parameter, D_P, which may be used as an indicator to represent the relative deflection stiffness due to the external wheel load and the loss of subgrade support:

$$D_P = \frac{Ph}{kl^4} = 12(1 - \mu^2)\frac{P}{Eh^2} \tag{13}$$

Thus, it was also hypothesized that the following six dimensionless parameters: a/l, L/l, W/l, $\alpha\Delta T$, D_γ, and D_P, would adequately describe the primary structural responses for the combination effect of loading plus thermal curling. To numerically validate this hypothesis, 16 ILLI-SLAB runs were performed and summarized in Table 2. While keeping these six parameters constant and changing any individual input variables, the resulting ILLI-SLAB edge stresses are proportional to the elastic modulus of the concrete slab. Thus, a unique edge strain was obtained as well.

The following equations (14) and (15) summarize the above relationships due to the effects of thermal curling alone and loading plus curling, respectively:

$$\frac{\sigma}{E}, \frac{\delta h}{l^2}, \frac{qh}{kl^2} = f\left(\alpha \Delta T, \frac{L}{l}, \frac{W}{l}, \frac{\gamma h^2}{kl^2}\right) \tag{14}$$

$$\frac{\sigma}{E}, \frac{\delta h}{l^2}, \frac{qh}{kl^2} = f\left(\frac{a}{l}, \alpha \Delta T, \frac{L}{l}, \frac{W}{l}, \frac{\gamma h^2}{kl^2}, \frac{Ph}{kl^4}\right) \tag{15}$$

Factorial Finite Element Runs

A series of finite element factorial runs were performed based on the dominating variables previously identified. Small BASIC PC programs were written to generate the finite element grids and input files to facilitate routine finite element analyses. The finite element mesh was designed according to the guidelines established in earlier studies (*12*). With the assistance of a file of batch commands, these factorial runs were performed as a background job on the HP/Apollo network. The desired results were automatically summarized to avoid untraced human errors.

NEW PREDICTIVE MODELING PROCEDURES

The proper selection of regression techniques is one of the most important factors to the success of prediction modeling. Traditional "**parametric**" regression techniques such as linear and nonlinear regressions require imposing a parametric form on the functions and then obtaining the parameter estimates afterwards. With the multi-dimensional pavement engineering problems in mind, several unresolved deficiencies were frequently identified in the use of traditional stepwise regression and nonlinear regression. These include problems in the selection of correct functional form, violations of the embedded statistical assumptions, and failure to satisfy some engineering boundary conditions.

In situations where little knowledge about the shape and the form of a function exists, several new "**nonparametric**" regression techniques developed over the past ten years have gradually gained popularity. Without imposing an unjustified parametric assumption, nonparametric regression techniques strive to estimate the actual functional form which best fits the data through the use of scatter plot smoothers (*14*).

The projection pursuit regression (PPR or "projection") algorithm introduced by Friedman and Stuetzle (*15*) appears to have the most favorable features due to its capability of handling variable interactions when suggesting transformations to improve the fit. The "projection" algorithm strives to model a multi-dimensional response surface as a sum of several projected curves through the use of local smoothing technique. The projected curves are essentially two-dimensional curves, which can be graphically displayed, easily visualized, and properly formulated. The relative importance of each projected curve can be measured by the absolute value of each coefficient associated with them as well.

A new statistical package named S-PLUS which has been widely used by statisticians for data analysis (*16, 17, 18, 19*) was selected due to the availability of this new regression technique. As a result, the following two-step modeling procedure was adopted (*20*):

1. Use the "projection" algorithm to break down the multi-dimensional response surface into a sum of several smooth projected curves; and
2. Use traditional linear and nonlinear regression techniques to obtain the parameter estimates of each individual projected curves and the overall regression statistics.

PREDICTIVE MODELS FOR LOADING ONLY

The effects of an external wheel loading subjected to a finite slab length and a finite slab width were analyzed separately. Adjustment (multiplication) factors for each individual effect were developed. Their combination effects can be approximately represented by multiplying both adjustment factors together.

Effect of Finite Slab Length

An adjustment factor (R_L) for the finite slab length effect was developed based on the following relationship:

$$R_L = \frac{\sigma_i}{\sigma_w} = f\left(\frac{a}{l}, \frac{L}{l}\right) \qquad \textbf{(16)}$$

Where:

σ_w = Westergaard's edge stress solution given in equation (1), [FL^{-2}]; and

σ_i = edge stress determined by the finite element model, [FL^{-2}].

Based on previous investigation (*7*), the maximum edge stress condition or Westergaard's infinite slab assumption may be achieved by selecting a value of 5.0 or more for the normalized slab length term (L/l). Thus, a more conservative value of 7.0 for both the normalized slab length and the normalized slab width (W/l) was selected to ensure an infinite slab condition. The following factorial finite element runs were performed:

a/l: 0.05, 0.10, 0.20, 0.30

L/l: 2.0, 2.5, 3.0, 3.5, 4.0, 4.5, 5.0, 6.0, 7.0

Note that W/l was remained a constant value of 7.0 for all runs. The pertinent input parameters of these factorial runs regarding load size, total wheel load, slab thickness, concrete modulus, and subgrade reaction are given in Table 3. The resulting ILLI-SLAB edge stresses when L/l = 7.0 and W/l = 7.0 were used to approximate Westergaard's solution in calculating adjustment factors. A three-dimensional perspective plot providing a very clear picture of the relationship among R_L, a/l, and L/l is shown in Figure 1 (a).

By using the aforementioned predictive modeling approach, the following one-term "projection" model was developed:

$$R_L = 0.9399 + 0.07986\,\Phi_1(ATX1) \qquad \textbf{(17)}$$

$$\Phi_1(ATX1) = -4.0308 + \frac{1}{0.2029 + 0.0345\,ATX1^{-3.3043}} \qquad \textbf{(18)}$$

$$ATX1 = -0.9436\frac{a}{l} + 0.3310\frac{L}{l} \tag{19}$$

Statistics: N = 36, R^2 = 0.994, SEE = 0.0063, CV = 0.67%

Limits: 2 ≤ L/l ≤ 7, 0.05 ≤ a/l ≤ 0.3

(Note: N = number of data points, R^2 = coefficient of determination, SEE = standard error of estimates, CV = coefficient of variation)

Effect of Finite Slab Width

The effect of finite slab width was often neglected in practice, since it is not as significant as the slab length effect. However, this effect as represented by the following adjustment factor (R_W) was considered in this study to have a more complete coverage on this topic:

$$R_W = \frac{\sigma_i}{\sigma_w} = f\left(\frac{a}{l}, \frac{W}{l}\right) \tag{20}$$

Thus, the following factorial ILLI-SLAB runs were performed:

a/l: 0.05, 0.10, 0.20, 0.30

W/l: 2.0, 2.5, 3.0, 3.5, 4.0, 4.5, 5.0, 6.0, 7.0

Note that L/l was kept a constant value of 7.0 for all runs. The pertinent input parameters were the same as before. A three-dimensional perspective plot for the relationship of R_W, *a/l*, and W/l is shown in Figure 1 (b). As expected, the slab width effect is not very significant. In fact, this effect is negligible when W/l is greater than 3 or 4. Besides, this effect is more pronounced for a pavement slab with a smaller W/l but a larger *a/l*.

Similarly, the following one-term "projection" model was developed:

$$R_W = 1.00477 + 0.01214\,\Phi_1(ATX1) \tag{21}$$

$$\Phi_1(ATX1) = -0.5344 + 1.6540(1 - ATX1)^{-10.7412} \tag{22}$$

$$ATX1 = 0.9951\frac{a}{l} - 0.09856\frac{W}{l} \tag{23}$$

Statistics: N = 36, R^2 = 0.947, SEE = 0.00299, CV = 0.30%

Limits: $2.0 \le W/l \le 7.0$, $0.05 \le a/l \le 0.3$

Due to limited number of runs performed and very narrow range of the adjustment factors obtained, this "projection" model was not as accurate as expected. However, it is relatively adequate for practical pavement design. With finer grids and more finite element runs performed, the above equations can be easily improved using the same modeling approach to achieve higher accuracy if necessary.

EFFECT OF THERMAL CURLING ONLY

The effect of a linear temperature differential and the finite extent of slab sizes must be considered together, since the principles of superposition can not be applied here. To account for the theoretical difference between Westergaard's solution and the finite element model, an adjustment factor (R_c) for curling may be defined as:

$$R_c = \frac{\sigma_i}{\sigma_c} = f\left(\alpha \Delta T \;,\; \frac{L}{l} \;,\; \frac{W}{l} \;,\; \frac{\gamma h^2}{k l^2}\right) \tag{24}$$

Where: σ_c = Westergaard/Bradbury's edge stress solution given in equation (9), [FL^{-2}].

Note that the adjustment factor introduced here is undefined when there is no temperature differential across the slab thickness. If temperature differentials are small, the ILLI-SLAB results due to day-time curling are approximately equal to those caused by night-time curling. The difference between them becomes substantial due to the combination effects of the self-weight of the concrete slab and the different extent of the loss of subgrade support caused by higher temperature differentials. Therefore, predictive models were separately developed for each day-time (positive ΔT) and night-time (negative ΔT) curling condition.

Preliminary Analysis

To investigate the combination effects of a linear temperature differential, a finite slab length, and a finite slab width, the following full factorial ILLI-SLAB runs were performed:

L/l: 3, 5, 7, 9, 11, 13, 15

W/l: 3, 5, 7, 9, 11, 13, 15

ΔT: ±10, ±20, ±30, ±40 °F

The symmetry option of the program was used to allow finer grids generated for the ILLI-SLAB runs. A constant slab thickness of 10.59 inches with an elastic concrete modulus of 5×10^6 psi over a subgrade having a k-value of 200 pci was also chosen for these runs. The coefficient of thermal expansion α was 5.5×10^{-6} /°F and the slab Poisson's ratio was 0.15. The unit weight of concrete slab (γ) was set to 0.087 pci since it is approximately constant in practice. (Note: 1 °F = (F - 32) / 1.8 °C, 1 inch = 2.54 cm, 1 psi = 6.89 kPa, 1 pci = 0.27 MN/m^3.)

The relationships among these variables and adjustment factors for day-time curling condition are displayed in Figure 2. Through the assistance of graphical displays, the overall trend and the individual adjustment factor can be easily identified. By this manner, any extraordinary behavior of the data may be located as well. As expected, the L/l requirement for an infinite slab condition is higher for higher temperature differentials. The theoretical discrepancy is higher for a shorter slab with a large negative temperature differential. Based on this investigation, those shorter slabs having both L/l and W/l equal to 3.0 were decided to be excluded from later predictive model development. It is mainly because numerical difficulties might arise while taking the ratio of small ILLI-SLAB results and small theoretical Westergaard solutions. Any approximation resulted from the ILLI-SLAB program might adversely affect the accuracy of the adjustment factors.

Attempts to develop predictive models using only these three important variables were not very successful. This was also the main reason which prompted us to search for an additional mechanistic variable as previously discussed.

Predictive Models for Thermal Curling Only

Additional ILLI-SLAB runs were apparently necessary since D_γ was remained constant unintentionally in the previous factorial runs, i.e., D_γ = 3.07E-05. Thus, the following full factorial finite element runs were performed:

W/*l*: 3, 7, 11

L/*l*: 3, 5, 7, 9, 11, 13, 15

ΔT: ±20, ±40 °F

D_γ: 0.78E-05, 6.13E-05, 11.03E-05

This was done by simply changing the unit weight of the concrete slab from previous 0.087 pci to 0.022, 0.174, and 0.313 pci (1 pci = 0.27 MN/m^3) while keeping all the rest of the input parameters the same as before. Together with those 392 cases previously analyzed, a total of 644 ILLI-SLAB runs which represented a partial factorial of these four dimensionless parameters were obtained to develop the following predictive models.

Generally speaking, the adjustment factor may be adequately defined by the sum of a series of projected curves using only these dimensionless parameters as independent variables. However, it was decided not to only rely upon the "projection" algorithm for modeling variable interactions in order to obtain the least number of projected curves for this high dimensional response surface (five dimensions). Some highly probable interaction terms were tested and included during the modeling process as well. By doing so, only a limited number of projected curves, which are more comprehensible to the user and can be easily formulated, are necessary for the model.

For day-time curling condition, the following two-term "projection" model was developed: (Note that a piece-wise linear model was chosen to represent these projected curves.)

$$R_c = 0.88369 + 0.22005\,\Phi_1(ATX1) + 0.02383\,\Phi_2(ATX2) \qquad \textbf{(25)}$$

$$\Phi_1(ATX1) = \begin{cases} -2.8903 + 2.7825\,ATX1 + 1.2565\,ATX1^2 & ,if\ ATX1 \le 0.85 \\ -2.4275 + 4.9285\,ATX1 - 1.9459\,ATX1^2 & ,if\ 0.85 < ATX1 \le 1.5 \\ 0.8111 - 0.1409\,ATX1 & ,if\ ATX1 > 1.5 \end{cases} \quad \textbf{(26)}$$

$$\Phi_2(ATX2) = \begin{cases} 2.3228 - 3.8187\,ATX2 - 52.8964\,ATX2^2 & ,if\ ATX2 \le -0.2 \\ -0.1891 - 0.2237\,ATX2 + 6.3312\,ATX2^2 & ,if\ -0.2 < ATX2 \le 0.6 \\ 25.7909 - 58.8336\,ATX2 + 32.4322\,ATX2^2 & ,if\ ATX2 > 10.6 \end{cases} \quad \textbf{(27)}$$

$$ATX1 = 0.00656\frac{W}{l} + 0.09886\frac{L}{l} - 0.02621\,ADT - 0.01857\,DG + 0.99456\log_{10}DG + 0.00129\,DG\frac{L}{l} \quad \textbf{(28)}$$

$$ATX2 = -0.00306\frac{W}{l} + 0.01649\frac{L}{l} + 0.02163\,ADT + 0.01336\,DG - 0.99953\log_{10}DG + 0.00413\,DG\frac{L}{l} \quad \textbf{(29)}$$

Statistics: N = 312, R^2 = 0.987, SEE = 0.0248, CV = 2.81%

Similarly, the following two-term "projection" model was developed for night-time curling condition:

$$R_c = 0.69811 + 0.36425\,\Phi_1(ATX1) + 0.03841\,\Phi_2(ATX2) \quad \textbf{(30)}$$

$$\Phi_2(ATX2) = \begin{cases} -0.5836 + 1.0057\,ATX2 + 0.9323\,ATX2^2 & ,if\ ATX2 \le 1 \\ -0.9296 + 2.2040\,ATX2 & ,if\ ATX2 > 1 \end{cases} \quad \textbf{(32)}$$

$$ATX1 = -0.02688\frac{W}{l} + 0.13185\frac{L}{l} + 0.04738\,ADT - 0.02553\,DG + 0.98938\log_{10}DG + 0.01089\,DG\frac{L}{l} \quad \textbf{(33)}$$

$$ATX2 = -0.14612\frac{W}{l} + 0.01252\frac{L}{l} - 0.10378\,ADT - 0.01890\,DG - 0.98355\log_{10}DG + 0.00053\,DG\frac{L}{l} \quad \textbf{(34)}$$

Statistics: N = 312, R^2 = 0.986, SEE = 0.0431, CV = 6.17%

Where: ADT = $\alpha\Delta T \times 10^5$, DG = $D_\gamma \times 10^5$.

Limits: $3 \le L/l \le 15$, $3 \le W/l \le 15$, $5.5 \le ADT \le 22$, $0.78 \le DG \le 11.03$

EFFECT OF LOADING PLUS THERMAL CURLING

The combination effects of loading and thermal curling can not be adequately described by simply superimposing the individual effects of loading and thermal curling alone, since the assumption of full contact condition between slab and subgrade is often violated. Thus, the following adjustment factor (R_T) was introduced to quantify this difference (2):

$$\sigma_i = \sigma_L + R_T \sigma_c \tag{35}$$

Together with knowledge of the dominating mechanistic variables involved, the adjustment factor may be determined by the following expression:

$$R_T = \frac{\sigma_i - \sigma_L}{\sigma_c} = f\left(\frac{a}{l},\ \alpha\Delta T,\ \frac{L}{l},\ \frac{W}{l},\ \frac{\gamma h^2}{k l^2},\ \frac{P h}{k l^4}\right) \tag{36}$$

Where:

σ_L = edge stress determined by the finite element model due to loading alone, which may be estimated by ($R_L * R_W * \sigma_w$), [FL^{-2}].

Preliminary Analysis

A preliminary analysis was conducted using the following four parameters: *a/l*, L/*l*, W/*l*, and $\alpha\Delta T$. The following full factorial ILLI-SLAB runs were performed:

a/l: 0.05, 0.1, 0.2, 0.3

L/*l*: 3, 5, 7, 9, 11, 13, 15

W/*l*: 3, 5, 7, 9, 11

ΔT: 0, ±20, ±40 °F

The pertinent input parameters are given in Table 3. Extreme difficulties were encountered while using only these four dimensionless parameters to develop a predictive model for the adjustment factor. Adding more interaction terms and more projected curves did not resolve this model inadequacy either. This problem also prompted us to search for the additional dimensionless mechanistic variables as previously discussed.

Predictive Models for Loading Plus Thermal Curling

To access the effect of all these six parameters on edge stress, it was necessary to perform additional ILLI-SLAB runs. However, a complete full factorial of these six parameters which requires a tremendous amount of computer time is not feasible. Thus, it was decided to generate a smaller supplemental factorial which could be added to the previous database to form a partial factorial for later model development. The data previously presented gave four D_γ values of 3.07E-05, 2.47E-05, 2.72E-05, and 2.52E-05, and four D_P values of 2.61E-05, 10.82E-05, 39.34E-05, and 114.40E-05, corresponding to four *a/l* values of 0.05, 0.1, 0.2, and 0.3. In other words, *a/l* and D_P were correlated with each other. To randomize the relationship among *a/l*, D_γ, and D_P, a smaller full factorial based on the following parameters was performed:

a/l: 0.05, 0.1, 0.2, 0.3
L/*l*: 3, 5, 7, 9, 11, 13, 15
W/*l*: 3, 7, 11
ΔT: 0, ±10, ±30 °F

This was done by changing unit weight of the concrete slab and total wheel load (or tire pressure) while keeping the other input parameters same as before for different *a/l* values. The pertinent input parameters are given in Table 4.

For the case of day-time curling plus loading, the following three-term "projection" model was developed:

$$R_T = 0.94825 + 0.15054\,\Phi_1(ATX1) + 0.03724\,\Phi_2(ATX2) + 0.03395\,\Phi_3(ATX3) \qquad \textbf{(37)}$$

$$\Phi_1(ATX1) = \begin{cases} -2.5575 + 0.8003\,ATX1 & ,if\ ATX1 \le 3 \\ -2.6338 + 1.1038\,ATX1 - 0.0914\,ATX1^2 & ,if\ 3 < ATX1 \le 7 \\ 0.7564 - 0.0155\,ATX1 & ,if\ ATX1 > 7 \end{cases} \quad \textbf{(38)}$$

$$\Phi_2(ATX2) = \begin{cases} -0.6788 + 0.0107\,ATX2 & ,if\ ATX2 \le 3 \\ 3.7674 - 2.2970\,ATX2 + 0.2963\,ATX2^2 & ,if\ 3 < ATX2 \le 7 \\ -7.0337 + 1.2945\,ATX2 & ,if\ ATX2 > 7 \end{cases} \quad \textbf{(39)}$$

$$\Phi_3(ATX3) = \begin{cases} 4.0843 + 4.8241\,ATX3 & ,if\ ATX3 \le -1 \\ 0.1815 + 0.0541\,ATX3 - 1.0899\,ATX3^2 & ,if\ -1 < ATX3 \le 0.5 \\ 0.0453 + 0.0383\,ATX3 & ,if\ ATX3 > 0.5 \end{cases} \quad \textbf{(40)}$$

$$\begin{aligned} ATX1 = & -0.04724\frac{W}{l} + 0.56954\frac{L}{l} - 0.08408\,ADT + 0.20033\frac{a}{l} \\ & -0.26647\,DG + 0.00375\,DP + 0.73881\frac{a}{l}\frac{L}{l} - 0.01142\,ADT\frac{L}{l} \\ & +0.09530\,DG\frac{L}{l} + 0.01121\,DG\frac{W}{l} \end{aligned} \quad \textbf{(41)}$$

$$\begin{aligned} ATX2 = & \ 0.03869\frac{W}{l} + 0.35781\frac{L}{l} + 0.09078\,ADT - 0.04054\frac{a}{l} \\ & +0.86388\,DG + 0.01635\,DP - 0.31246\frac{a}{l}\frac{L}{l} + 0.00552\,ADT\frac{L}{l} \\ & -0.12677\,DG\frac{L}{l} - 0.01765\,DG\frac{W}{l} \end{aligned} \quad \textbf{(42)}$$

$$\begin{aligned} ATX3 = & \ 0.58567\frac{W}{l} + 0.25804\frac{L}{l} + 0.14784\,ADT + 0.14984\frac{a}{l} \\ & +0.12743\,DG - 0.05012\,DP + 0.72295\frac{a}{l}\frac{L}{l} - 0.01310\,ADT\frac{L}{l} \\ & -0.01304\,DG\frac{L}{l} - 0.06591\,DG\frac{W}{l} \end{aligned} \quad \textbf{(43)}$$

Statistics: N = 432, R^2 = 0.970, SEE = 0.0280, CV = 2.95%

Similarly, the following three-term "projection" model was developed for the case of night-time curling plus loading:

$$R_T = 0.76068 + 0.28490\,\Phi_1(ATX1) + 0.10707\,\Phi_2(ATX2) + 0.10048\,\Phi_3(ATX3) \quad \textbf{(44)}$$

$$\Phi_1(ATX1) = \begin{cases} -2.5301 + 0.3866\,ATX1 & ,if\ ATX1 \le 6 \\ -4.0938 + 0.8799\,ATX1 - 0.0395\,ATX1^2 & ,if\ 6 < ATX1 \le 12 \\ 0.3181 + 0.0435\,ATX1 & ,if\ ATX1 > 12 \end{cases} \quad \textbf{(45)}$$

$$\Phi_2(ATX2) = \begin{cases} -1.4980 - 1.1359\,ATX2 & ,if\ ATX2 \le -1 \\ -0.4956 - 0.0892\,ATX2 + 0.0174\,ATX2^2 & ,if\ -1 < ATX2 \le 5 \\ -1.1278 + 0.1075\,ATX2 & ,if\ ATX2 > 5 \end{cases} \quad \textbf{(46)}$$

$$\Phi_3(ATX3) = \begin{cases} 3.6341 + 0.6512\,ATX3 & ,if\ ATX3 \le -7 \\ -\ 0.2683 - 0.6808\,ATX3 - 0.1116\,ATX3^2 & ,if\ -7 < ATX3 \le -1 \\ 0.1966 - 0.2061\,ATX3 & ,if\ ATX3 > -1 \end{cases} \tag{47}$$

$$\begin{aligned} ATX1 = & -0.13971\frac{W}{l} + 0.85779\frac{L}{l} + 0.07003\,ADT + 0.19562\frac{a}{l} \\ & + 0.36589\,DG + 0.05950\,DP - 0.24211\frac{a}{l}\frac{L}{l} + 0.07242\,DG\frac{L}{l} \\ & - 0.00482\,DP\frac{L}{l} + 0.00797\,ADT\frac{L}{l} + 0.01220\,ADT\frac{W}{l} \end{aligned} \tag{48}$$

$$\begin{aligned} ATX2 = & -0.15106\frac{W}{l} + 0.08443\frac{L}{l} + 0.28234\,ADT - 0.48812\frac{a}{l} \\ & + 0.17449\,DG - 0.03194\,DP - 0.78445\frac{a}{l}\frac{L}{l} - 0.01999\,DG\frac{L}{l} \\ & + 0.00206\,DP\frac{L}{l} - 0.06949\,ADT\frac{L}{l} - 0.00419\,ADT\frac{W}{l} \end{aligned} \tag{49}$$

$$\begin{aligned} ATX3 = & \ 0.10960\frac{W}{l} - 0.60315\frac{L}{l} - 0.26836\,ADT + 0.06965\frac{a}{l} \\ & - 0.71547\,DG - 0.12704\,DP + 0.02846\frac{a}{l}\frac{L}{l} + 0.13364\,DG\frac{L}{l} \\ & + 0.01088\,DP\frac{L}{l} + 0.02248\,ADT\frac{L}{l} + 0.00260\,ADT\frac{W}{l} \end{aligned} \tag{50}$$

Statistics: N = 432, R^2 = 0.961, SEE = 0.0546, CV = 7.17%

Where: ADT = $\alpha\Delta T \times 10^5$, DG = $D_\gamma \times 10^5$, DP = $D_P \times 10^5$.

Limits: $0.05 \le a/l \le 0.30$, $3 \le L/l \le 15$, $3 \le W/l \le 11$,

$5.5 \le ADT \le 22$, $1.06 \le DG \le 9.93$, $2.61 \le DP \le 140.74$

VALIDATION OF THE PROPOSED PREDICTIVE MODELS

To further validate the applicability of the developed predictive models, a series of ILLI-SLAB factorial runs were performed based on a wide range of input parameters. These factorial runs were totally independent of the previous modeling process. The following input parameters covering most of the practical cases found in the field were selected:

Elastic modulus of the concrete, E = 3.0, 5.5, 8.0 Mpsi;

Modulus of subgrade reaction, k = 50, 250, 500 pci;

Slab length, L = 10, 20, 30 ft;

Slab thickness, h = 8, 12, 16 in.; and

Temperature differential, $\Delta T = \pm 20, \pm 40$ °F.

(Note: 1 psi = 6.89 kPa, 1 pci = 0.27 MN/m^3, 1 ft = 30.48 cm, 1 °F = (F - 32) / 1.8 °C.)

The above factorial runs (324 runs) were performed for the case of curling only without external wheel load applied. The width of the slab was 12 feet, the slab Poisson's ratio was 0.15, the coefficient of thermal expansion was 5.5×10^{-6} /°F, and the unit weight of concrete slab was set to 0.087 pci.

For the case of loading only, a wheel load of 9,000 pounds (40 KN) was applied to the 10-ft slabs whereas an 18,000-pound (80 KN) load was applied to the other 20-ft and 30-ft slabs. The tire pressure was set to 90 psi. Thus, a single loaded rectangle of the size of 10 x 10 or 20 x 10 in^2 was used for the 10-ft slabs or 20-ft and 30-ft slabs, respectively. Therefore, only 81 ILLI-SLAB runs were performed. As for the case of loading and curling, a total of 324 runs similar to the case of curling only but with the wheel loads were performed.

Thus, the above factorials essentially result in a group of pavement slabs whose data ranges are a/l = 0.07 to 0.35, L/l = 1.4 to 15.9, W/l = 1.7 to 6.4, $\alpha\Delta T$ = -0.00022 to 0.00022, D_γ = 1.3E-05 to 9.7E-05, and D_P = 5.2E-05 to 110.0E-05. To examine the applicability of the predictive models to pavement slabs with any other input parameters, some of the data points which are outside of the specified limits of the proposed predictive models were not considered.

The adequacy of the proposed predictive models for the effects of loading alone, thermal curling alone, and loading plus curling were further validated using the above factorial data. The predicted edge stresses are plotted against the actual values as shown in Figure 3 (a), (b) and (c), respectively. Clearly, these predictive models were able to make fairly good prediction for these data. Thus, it further reconfirmed the applicability of the proposed predictive models.

CALCULATED VERSUS MEASURED STRESSES

The edge stresses computed by the proposed predictive models were compared to the actual measured stress from the AASHO Road Test (*21*) and the Arlington Road Test (*10*). Favorable agreements (*20*) have also been achieved for the three cases analyzed.

NUMERICAL EXAMPLES

Consider a pavement slab with the following characteristics: E = 5.5 Mpsi, k = 250 pci, L = 10 ft, W = 12 ft, h = 12 in., γ = 0.087 pci, μ = 0.15, and $\alpha = 5.5 \times 10^{-6}$ /ºF. A single wheel load of 9,000 lbs with a loaded rectangle of the size of 10 x 10 in^2 is applied. A linear temperature differential of +20 ºF (day-time condition) exists through the slab thickness. Determine the critical edge stresses due to loading alone, curling alone, and loading plus curling. (Note: 1 psi = 6.89 kPa, 1 pci = 0.27 MN/m^3, 1 ft = 30.48 cm, 1 in. = 2.54 cm, 1 ºF = (F - 32) / 1.8 ºC, 1 lb = 4.45 N.)

The equivalent radius of the loaded area is a = 5.64 in. and the radius of relative stiffness of the slab-subgrade system is l = 31.20 in. Therefore, the actual dominating mechanistic variables are a/l = 0.18, L/l = 3.83, W/l = 4.60, $\alpha\Delta T$ = +11.0E-05, D_γ = 2.27E-05, and D_P = 29.99E-05. The theoretical Westergaard's solutions based on equations (1) and (9) are σ_w = 345.75 psi and σ_c = 118.25 psi for loading only and curling only, respectively.

For the case of loading only, the adjustment factors for finite slab length and width are R_L = 0.968 and R_W = 1.000 using equations (17) and (21), respectively. Thus, the edge stress determined by the proposed models is 0.968 x 1.000 x 345.75 = 334.7 psi. (Note that the actual ILLI-SLAB edge stress was 344.36 psi.)

For the case of curling only, the adjustment factor is R_c = 0.570, which is determined by equation (25). This gives a predicted edge stress of 118.25 x 0.570 = 67.40 psi. (Note that the actual ILLI-SLAB edge stress was 68.4 psi.)

For the case of loading plus curling, the adjustment factor is R_T = 0.732 based on equation (37). Thus, the predicted total edge stress determined by the proposed model is 334.7 + 0.732 x 118.25 = 421.3 psi using equation (35). (Note that the actual ILLI-SLAB edge stress was 436.42 psi for this case.)

CONCLUSIONS

The edge stress of a concrete pavement due to the individual and combination effects of a single wheel load and a linear temperature differential across the slab thickness was conducted under this study. The subgrade was assumed to act as a dense liquid foundation.

Based on previous research using dimensional analysis, the major independent variables were: normalized load radius (*a/l*), normalized slab length (L/*l*), normalized slab width (W/*l*), and a dimensionless product ($\alpha\Delta T$) of a temperature differential and thermal expansion coefficient. However, using only these four parameters the actual structural response to a temperature influence could not be described adequately. Fortunately, two additional dimensionless parameters (D_γ and D_P) representing the relative deflection stiffness due to the self-weight of the concrete slab, the applied load, and the possible loss of support were recently identified. With this discovery, the problems encountered in previous investigations (*1*) using dimensional analysis for thermal-related curling problems are now resolved.

A new predictive modeling procedure proposed by Lee (*20*), which makes use of the projection pursuit regression (PPR or "projection") algorithm, traditional linear and nonlinear regression techniques, was utilized to develop the proposed models. The new models use only the dominating mechanistic variables as opposed to earlier attempts using arbitrary linear combination of input parameters with very few insights to the actual relationships among the variables. Consequently, three closed-form mechanistic design models which have been carefully validated and ready for implementation on a spreadsheet or computer program were presented. These stress models turned out to be very accurate representations of the finite element model.

The new models were also properly formulated to satisfy applicable engineering boundary conditions. They are also simple, easy to comprehend, dimensionally correct, and may be extrapolated to wider ranges of other input parameters. Practical numerical examples showing the use of the new models are also provided.

The predictive models cover almost all practical ranges of pavement designs. Since they are dimensionally correct, they can be used in any other unit systems as well. However, extrapolation outside the specified ranges of these dominating parameters is not recommended. Practical pavement design guidelines for edge stress analysis may be easily developed based on these predictive models together with the use of some reliability concepts. Besides, the predictive modeling procedures and the "deflection-ratio" concept may be utilized in other pavement related modeling problems as well.

ACKNOWLEDGMENTS

This research work was sponsored by the Illinois Department of Transportation. The authors are grateful to Mr. James Hall for his assistance in this project.

REFERENCES

1. Salsilli-Murua, R. A. (1991). "Calibrated Mechanistic Design Procedure For Jointed Plain Concrete Pavements." Ph.D. Thesis, University of Illinois, Urbana.
2. Darter, M. I. (1977). "Design of Zero-Maintenance Plain Jointed Concrete Pavement, Vol. I - Development of Design Procedures." Federal Highway Administration Report No. FHWA-RD-77-111, Washington, D.C.
3. Westergaard, H. M. (1926[a]). "Computation of Stresses in Concrete Roads." Proceedings of the Fifth Annual Meeting, Vol. 5, Part I, Highway Research Board, pp. 90-112. Also in "Stresses in Concrete Pavements Computed by Theoretical Analysis." Public Roads, Vol.7, No. 2, April, 1926, pp. 25-35.
4. Westergaard, H. M. (1943). "Stresses Concentrations in Plates Loaded over Small Areas." American Society of Civil Engineers, Transactions, Vol. 108, pp. 831-886. Also in ASCE Proceedings, Vol. 68, No. 4, April, 1942.

5. Westergaard, H. M. (1948). "New Formulas for Stresses in Concrete Pavements of Airfields." American Society of Civil Engineers, Transactions, Vol. 113, pp. 425-444. Also in ASCE Proceedings, Vol. 73, No. 5, May, 1947.

6. Ioannides, A. M. and R. A. Salsilli-Murua (1989). "Temperature Curling in Rigid Pavements: An Application of Dimensional Analysis." Transportation Research Record 1227, Transportation Research Board, Washington, D.C.

7. Ioannides, A. M., M. R. Thompson, and E. J. Barenberg (1985). "The Westergaard Solutions Reconsidered." Transportation Research Record 1043, Transportation Research Board.

8. Westergaard, H. M. (1926[b]). "Analysis of Stresses in Concrete Pavements due to Variations of Temperature." Proceedings, Vol. 6, Highway Research Board, pp. 201-217. Also in Public Roads, Vol. 8, No. 3, May 1927.

9. Bradbury, R. D. (1938). Reinforced Concrete Pavements. Wire Reinforcement Institute, Washington, D.C.

10. Teller, L. W. and E. C. Sutherland (1935). "The Structural Design of Concrete Pavements." Part 2, Public Roads, Vol. 16, No. 9, November.

11. Tabatabaie-Raissi, A. M. (1978). "Structural Analysis of Concrete Pavement Joints." Ph.D. Thesis, University of Illinois, Urbana.

12. Ioannides, A. M. (1984). "Analysis of Slabs-on-Grade for a Variety of Loading and Support Conditions." Ph.D. Thesis, University of Illinois, Urbana.

13. Korovesis, G. T. (1990). "Analysis of Slab-on-Grade Pavement Systems Subjected to Wheel and Temperature Loadings." Ph.D. Thesis, University of Illinois, Urbana.

14. Hastie, T. J. and R. J. Tibshirani (1990). Generalized Additive Models. Monographs on Statistics and Applied Progability 43, Chapman and Hall.

15. Friedman, J. H. and W. Stuetzle (1981). "Projection Pursuit Regression." Journal of the American Statistical Association, Vol. 76, pp. 817-823.

16. Becker, R. A., J. M. Chambers, and A. R. Wilks (1988). The New S Language - A Programming Environment for Data Analysis and Graphics. The Wadsworth & Brooks/Cole Computer Science Series, AT&T Bell Laboratories.

17. Statistical Sciences, Inc. (1991[a]). S-PLUS for DOS: Reference Manual. Version 2.0, Seattle, Washington, November.

18. Statistical Sciences, Inc. (1991[b]). S-PLUS for DOS: User's Manual. Version 2.0, Vol. 1 and Vol. 2, Seattle, Washington, November.

19. Chambers, J. M. and T. J. Hastie (1992). Statistical Models in S. Wadsworth & Brooks/Cole Computer Science Series, AT&T Bell Laboratories.

20. Lee, Y. H. (1993). "Development of Pavement Prediction Models." Ph.D. Thesis, University of Illinois, Urbana.

21. Highway Research Board (1962). "The AASHO Road Test." Report 5, Pavement Research, Special Report 61E, Publication No. 954, Washington, D.C.

Table 1 - ILLI-SLAB Runs: An Additional Parameter (D_γ) for Curling Only

ΔT °F	h in.	E Mpsi	k pci	L in.	W in.	α $x10^{-6}$	γ pci	σ_i psi
16	8.47	39.94	51	398.94	398.94	6.88	0.136	1156.576
16	21.18	2.56	51	398.94	398.94	6.88	0.022	74.405
40	8.47	39.94	51	398.94	398.94	2.75	0.136	1156.132
40	21.18	2.56	51	398.94	398.94	2.75	0.022	74.376
16	8.47	19.97	102	282.09	282.09	6.88	0.136	578.046
16	21.18	1.28	102	282.09	282.09	6.88	0.022	37.179
40	8.47	19.97	102	282.09	282.09	2.75	0.136	577.815
40	21.18	1.28	102	282.09	282.09	2.75	0.022	37.164
16	8.47	4.99	409	141.05	141.05	6.88	0.136	145.151
16	21.18	0.32	409	141.05	141.05	6.88	0.022	9.339
40	8.47	4.99	409	141.05	141.05	2.75	0.136	145.095
40	21.18	0.32	409	141.05	141.05	2.75	0.022	9.335
16	8.47	2.22	920	94.03	94.03	6.88	0.136	64.563
16	21.18	0.14	920	94.03	94.03	6.88	0.022	4.139
40	8.47	2.22	920	94.03	94.03	2.75	0.136	64.539
40	21.18	0.14	920	94.03	94.03	2.75	0.022	4.138

Note:

1. $L/l = 5.0$, $W/l = 5.0$, $\alpha\Delta T = 1.1E-04$, $D_\gamma = 3.0E-05$, $\mu = 0.15$.
2. 1 °F = (F − 32) / 1.8 °C, 1 inch = 2.54 cm, 1 psi = 6.89 kPa, 1 pci = 0.27 MN/m^3.

Table 2 - ILLI-SLAB Runs: Two Additional Parameters (D_γ and D_P) for Loading Plus Curling

c in.	P lbs	ΔT °F	h in.	E Mpsi	k pci	L in.	W in.	α x10^{-6}	γ pci	σ_i psi
2.5*	1833	16	8.47	9.99	204.35	119.68	159.58	6.88	0.136	172.266
2.5*	733	16	21.18	0.64	204.35	119.68	159.58	6.88	0.022	11.039
2.5*	1833	40	8.47	9.99	204.35	119.68	159.58	2.75	0.136	172.239
2.5*	733	40	21.18	0.64	204.35	119.68	159.58	2.75	0.022	11.038
5.0	3666	16	8.47	19.97	102.17	169.26	225.68	6.88	0.136	344.294
5.0	1466	16	21.18	1.28	102.17	169.26	225.68	6.88	0.022	22.063
5.0	3666	40	8.47	19.97	102.17	169.26	225.68	2.75	0.136	344.239
5.0	1466	40	21.18	1.28	102.17	169.26	225.68	2.75	0.022	22.060
7.5	8248	16	8.47	44.93	45.41	253.89	338.51	6.88	0.136	773.457
7.5	3299	16	21.18	2.88	45.41	253.89	338.51	6.88	0.022	49.565
7.5	8248	40	8.47	44.93	45.41	253.89	338.51	2.75	0.136	773.335
7.5	3299	40	21.18	2.88	45.41	253.89	338.51	2.75	0.022	49.557
10.0	14663	16	8.47	79.88	25.54	338.51	451.35	6.88	0.136	1360.855
10.0	5865	16	21.18	5.11	25.54	338.51	451.35	6.88	0.022	87.211
10.0	14663	40	8.47	79.88	25.54	338.51	451.35	2.75	0.136	1360.642
10.0	5865	40	21.18	5.11	25.54	338.51	451.35	2.75	0.022	87.197

Note:

1. Load dimensions are c x c, except those starred cases use 2c x c. L/l = 3.0, W/l = 4.0, $\alpha\Delta T$ = 1.1E-04, D_γ = 3.0E-05, D_P = 3.0E-05, μ = 0.15.
2. 1 °F = (F - 32) / 1.8 °C, 1 lb = 4.45 N, 1 inch = 2.54 cm, 1 psi = 6.89 kPa, 1 pci = 0.27 MN/m^3.

Table 3 - Pertinent Input Parameters for Loading and Loading Plus Curling

a/l	c in.	*a* in.	E Mpsi	k pci	h in.	*l* in.	P lbs	DG	DP
0.05	2.5*	1.995	5	200	10.59	39.89	1250	3.07	2.61
0.10	5.0	2.821	4	300	8.23	28.21	2500	2.47	10.82
0.20	10.0	5.642	3	400	9.97	28.21	10000	2.72	39.34
0.30	10.0	5.642	2	500	7.16	18.81	10000	2.52	114.40

Note:

1. Load dimensions are c x c, except those starred cases use 2c x c. α = 5.5E-06 /°F, μ = 0.15, γ = 0.087 pci, p = 100 psi, DG = $D_\gamma \times 10^5$, DP = $D_P \times 10^5$.
2. 1 °F = (F - 32) / 1.8 °C, 1 lb = 4.45 N, 1 inch = 2.54 cm, 1 psi = 6.89 kPa, 1 pci = 0.27 MN/m^3.

Table 4 - Pertinent Input Parameters for Loading Plus Curling (Additional Runs)

a/l	c in.	*a* in.	E Mpsi	k pci	h in.	*l* in.	γ pci	p psi	P lbs	DG	DP
0.05	2.5*	1.995	5	200	10.59	39.89	0.030	5000	62500	1.06	130.74
0.10	5.0	2.821	4	300	8.23	28.21	0.350	600	15000	9.93	64.94
0.20	10.0	5.642	3	400	9.97	28.21	0.170	250	25000	5.31	98.34
0.30	10.0	5.642	2	500	7.16	18.81	0.300	10	1000	8.69	11.44

Note:

1. Load dimensions are c x c, except those starred cases use 2c x c. α = 5.5E-06 /°F, μ = 0.15, DG = $D_\gamma \times 10^5$, DP = $D_P \times 10^5$.
2. 1 °F = (F - 32) / 1.8 °C, 1 lb = 4.45 N, 1 inch = 2.54 cm, 1 psi = 6.89 kPa, 1 pci = 0.27 MN/m^3.

Figure 1 (a) - Finite Slab Length Effect

Figure 1 (b) - Finite Slab Width Effect

Figure 2 - Effects of a Positive Temperature Differential and Finite Slab Size

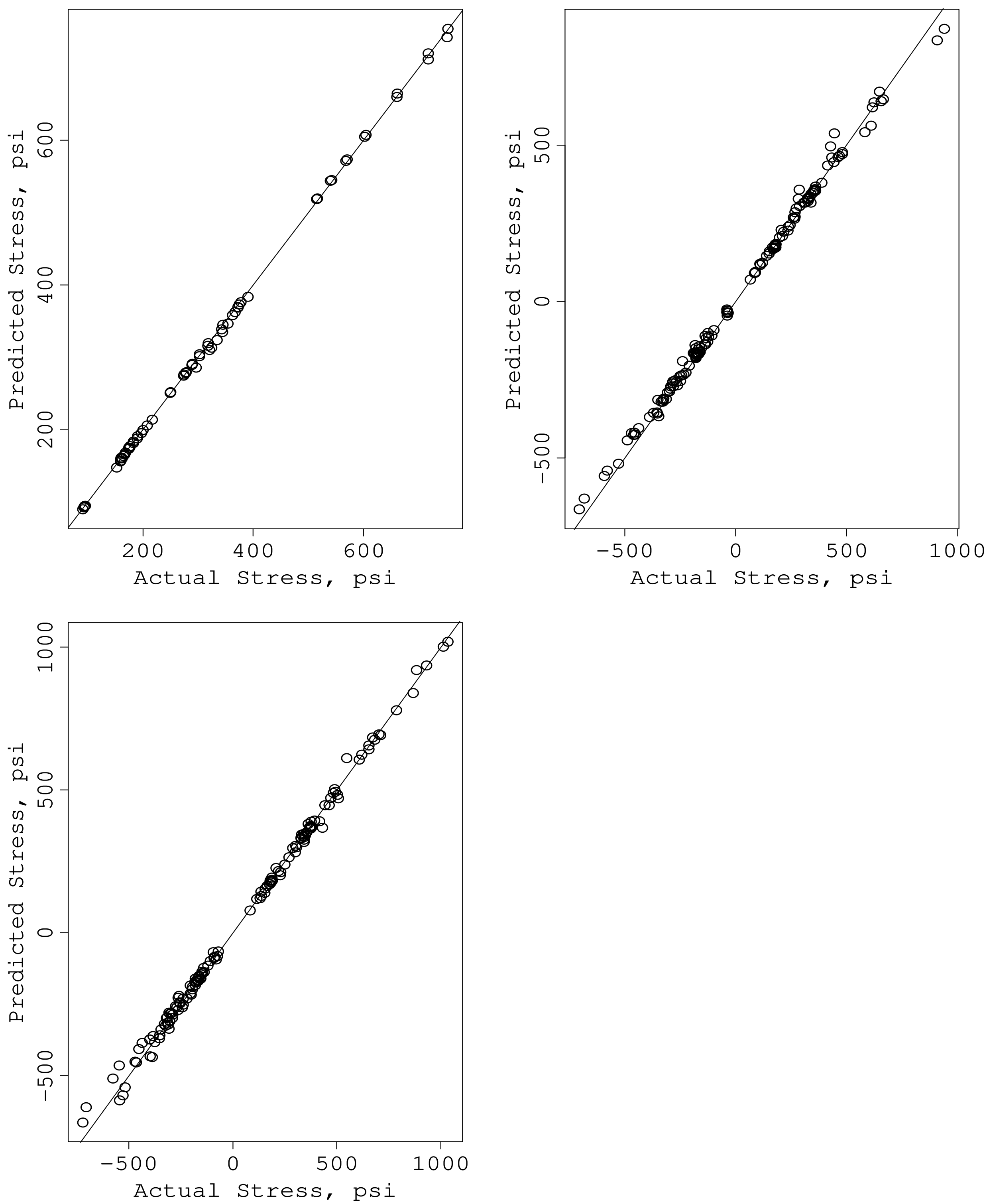

Figure 3 - Validation of the Proposed Models for: (a) Loading Only, (b) Curling Only, and (c) Loading Plus Curling